LAWRENCE
LIVERMORE
NATIONAL
LABORATORY

UCRL-JRNL-207613

Laser-Activated Shape Memory Polymer Microactuator for Thrombus Removal Following Ischemic Stroke

W. Small IV, M. F. Metzger, T. S. Wilson, D. J. Maitland

November 1, 2004

IEEE Journal of Selected Topics in Quantum Electronics

Laser-Activated Shape Memory Polymer Microactuator for Thrombus Removal Following Ischemic Stroke: Preliminary *In Vitro* Analysis

Ward Small IV, Melodie F. Metzger, Thomas S. Wilson, Duncan J. Maitland

This work was performed under the auspices of the U.S. Department of Energy by University of California, Lawrence Livermore National Laboratory under Contract W-7405-ENG-48 and supported by the National Institutes of Health/National Institute of Biomedical Imaging and Bioengineering, Grant R01EB000462.

W. Small IV, T. S. Wilson, and D. J. Maitland are with Lawrence Livermore National Laboratory, Livermore, CA 94550 USA.

M. F. Metzger is with Sierra Interventions, LLC, Berkeley, CA 94705 USA

Abstract-- Due to the narrow (3-hour) treatment window for effective use of the thrombolytic drug recombinant tissue-type plasminogen activator (rt-PA), there is a need to develop alternative treatments for ischemic stroke. We are developing an intravascular device for mechanical thrombus removal using shape memory polymer (SMP). We propose to deliver the SMP microactuator in its secondary straight rod form (length = 4 cm, diameter = 350 μm) through a catheter distal to the vascular occlusion. The microactuator, which is mounted on the end of an optical fiber, is then transformed into its primary corkscrew shape by laser heating (diode laser, λ = 800 nm) above its soft phase glass transition temperature (T_{gs} = 55°C). Once deployed, the microactuator is retracted and the captured thrombus is removed to restore blood flow. The SMP is doped with indocyanine green (ICG) dye to increase absorption of the laser light. Successful deployment of the microactuator depends on the optical properties of the ICG-doped SMP and the optical coupling efficiency of the interface between the optical fiber and the SMP. Spectrophotometry, thermal imaging, and computer simulation aided the initial design effort and continue to be useful tools for optimization of the dye concentration and laser power. Thermomechanical testing was performed to characterize the elastic modulus of the SMP. We have demonstrated laser-activation of the SMP microactuator in air at room temperature, suggesting this concept is a promising therapeutic alternative to rt-PA.

Keywords: diode laser, shape memory polymer, ischemic stroke, indocyanine green

I. INTRODUCTION

Conventional treatment for acute ischemic stroke is intravenous administration of recombinant tissue-type plasminogen activator (rt-PA). This thrombolytic drug, which is infused over a 1 hour period, restores blood flow by chemically dissolving the thrombus following ischemic stroke. A Phase III multicenter clinical trial demonstrated beneficial outcomes when rt-PA was administered within 3 hours of the onset of stroke symptoms [1], though patients treated within 90 minutes showed the most benefit [2]. In a separate

Phase III trial, patients treated 3-5 hours after symptom onset showed no benefit [3], confirming that rt-PA should only be administered within 3 hours. However, the majority of patients are not eligible to receive intravenous rt-PA, mainly due to delays in obtaining treatment [4]. Additional drawbacks of rt-PA include the relatively high risk of intracranial hemorrhage, the numerous contraindications prohibiting treatment, and the extensive patient follow-up monitoring and care associated with systemic thrombolytic drug exposure [1].

A potential alternative to rt-PA is mechanical removal of the thrombus using a micro-device deployed endovascularly. Shape memory polymer (SMP) has been identified as a material suitable for therapeutic microactuator fabrication [5], [6]. We are developing a catheter-based SMP device to capture and remove the thrombus and restore blood flow following ischemic stroke. The proposed concept is illustrated in Fig. 1. SMP is a unique polyurethane-based material that can maintain a stable secondary shape and, upon controlled heating, will return to its primary shape. In our device, the primary shape is a tapered corkscrew shape and the secondary shape is a straight rod. We propose to deliver the SMP microactuator in its secondary straight rod form through a catheter distal to the vascular occlusion. The microactuator, which is mounted on the end of an optical fiber, is then transformed into its primary corkscrew shape by laser heating. Once deployed, the microactuator is retracted and the captured thrombus is removed from the body to restore blood flow. In this paper, we describe the operation of the SMP device and the methods used to select and characterize its optical properties for laser heating. We also report preliminary results of "proof-of-principle" benchtop laser actuation. This study has established the framework for future device optimization.

II. MATERIALS AND METHODS

A. Shape Memory Effect

The device was fabricated using a commercially available thermoplastic SMP (MM5520, DiAPLEX Company, Ltd., a subsidiary of Mitsubishi Heavy Industries, Ltd., Tokyo, Japan). Recovery of the stable primary shape is achieved by controlled heating of the SMP in its stable secondary shape. While heated above its highest glass transition temperature ($T_g \approx 130°C$), the SMP is formed into the primary shape and cooled to stabilize the shape. At a temperature above its soft phase glass transition temperature ($T_{gs} = 55°C$), the SMP is deformed into a secondary shape and then cooled. The primary shape is recovered by heating again to T_{gs}.

B. Microactuator Fabrication

The raw SMP material was extruded into a strand with circular cross-section approximately 350 μm in diameter. A cylindrical rod segment approximately 4 cm in length was obtained. In one end of the segment, a hole (diameter = 127 μm, depth = 1 mm) was drilled coaxial with the longitudinal axis of the rod. A multimode ultra low-OH

100 μm core diameter (125 μm diameter including the polyimide buffer) step-index silica core/silica clad optical fiber (FIP100110125, Polymicro Technologies, Phoenix, AZ) was cleaved on one end (numerical aperture = 0.22). The other end (terminated with an ST connector) was coupled to a pigtailed 800 nm diode laser (H01-A001-800-FC/100, Opto Power Corporation, Tucson, AZ). The cleaved end of the fiber was inserted into the drilled socket in the SMP rod and secured with a fast-setting epoxy (Double-Bubble Red #04001, Hardman, Inc., Belleville, NJ) around the joint. The tip of the drill bit used to create the socket was slightly convex, resulting in a small air gap between the cleaved fiber tip and the SMP. A microscope image of the fiber-SMP joint is shown in Fig. 2 and a schematic representation of the joint configuration is shown in Fig. 3.

After the epoxy was fully cured, the SMP rod was wrapped around a cone-shaped aluminum mandrel fabricated in-house to set the primary corkscrew shape. A narrow channel machined around the mandrel and an aluminum cap placed over the mandrel captured the wrapped SMP rod and maintained the corkscrew form during the heating procedure. The mandrel assembly was placed in a hot air stream (Model 185-A, Beahm Designs, Los Gatos, CA) at approximately 130°C for 15-20 minutes and then cooled to room temperature to set the primary shape. The SMP microactuator is shown in its corkscrew form in Fig. 4. The corkscrew shape was chosen to maintain the waveguiding ability of the SMP microactuator while providing a means of capturing a thrombus. After removing the SMP from the mandrel, it was placed in the hot air stream at approximately 75°C and manually straightened into its secondary rod shape, and then cooled to set the secondary shape prior to laser actuation.

C. Laser-SMP Optical Coupling

The circular cross-section of the SMP microactuator enhances its waveguiding ability, enabling light to propagate along its entire length with minimal loss due to leakage. In order to increase absorption of the 800 nm diode laser light and enhance heating, the SMP rods were doped with indocyanine green (ICG) dye (Sigma Chemical Co., St. Louis, MO) which has a strong absorption peak near 800 nm. Prior to drilling the hole in the SMP rod, the rod was soaked in a solution of ICG dye and methanol, allowing the ICG dye to diffuse into the SMP, and then vacuum dried to remove the methanol. The concentration of ICG in the SMP rod was estimated based on the ICG concentration in the methanol and amount of methanol that diffused into the SMP; the ICG concentration in the SMP was assumed to be uniform. Rods with ICG concentrations from approximately 0.08 to 4.7 μM were made.

D. Spectrophotometry

The absorption coefficient of the ICG-doped SMP was calculated for various ICG concentrations. Using a spectrophotometer (Cary 300, Varian Instruments, Walnut Creek, CA), the spectral absorbance of thin samples of thermoset SMP (MP5510, DiAPLEX Company, Ltd.) with various ICG dye concentrations (0-40.6 μM) was measured. The

thermoset material, which is easily molded into thin films unlike the thermoplastic material used for the device, was used to facilitate fabrication of the samples. Also, because it is in a liquid state prior to curing, the ICG dye was added directly to the uncured material, allowing uniform distribution of the dye and accurate control of the concentration. After removing the contribution from reflective losses inherent in the measurement, the absorbance data were used to calculate the absorption coefficient, μ_a, at the laser wavelength (800 nm) as a function of ICG dye concentration:

$$\mu_a = \frac{A}{d} \ln 10 \tag{1}$$

where A is the absorbance, d is the sample thickness, and ln is the natural logarithm (ln10 = 2.303). The absorption coefficient varies linearly with absorbance. Equation (1) was derived from the equations relating the fraction of transmitted light, T, to A and μ_a: $A=\log_{10}(1/T)$ and $T=\exp(-\mu_a d)$ [7].

In order to estimate the absorption of ICG-doped thermoplastic, the absorbance of a thin sample of thermoplastic SMP without dye was measured. Because the absorbance value at 800 nm was within the noise level of the measurement (*i.e.,* reflective losses exceeded actual absorption), it was estimated to be zero. In contrast, the thermoset material without dye had measurable (nonzero) absorbance at 800 nm. Assuming the dependence of absorbance on dye concentration is the same for thermoplastic and thermoset SMP, the thermoset absorption coefficient versus dye concentration curve was simply shifted down to intercept the origin to estimate the thermoplastic absorption.

Because the photon mean free path (*i.e.,* the average distance a photon will travel before being absorbed, ignoring scattering) is simply the reciprocal of the absorption coefficient, the absorption coefficient provides information regarding the penetration depth of the light in ICG-doped SMP. The contribution of scattering to the overall attenuation of the light was assumed to be insignificant with respect to that of ICG absorption. Scattering in the SMP device is negligible by design. The SMP rod extrusion, which is similar to methods used to extrude polymer optical fibers, was controlled to produce rod stock without any significant scattering contributions, which include bubbles, large crystalline phase inclusions, or contaminant inclusions. Furthermore, Rayleigh scattering induced by density fluctuations in the SMP during the extrusion process is particularly low for 800 nm light since it is inversely proportional to the fourth power of the wavelength. Ignoring loss mechanisms other than absorption, the amount of light decreases exponentially with distance into the SMP:

$$T = \exp\left(-\mu_a d\right) \tag{2}$$

where T is the fraction of light transmitted and d is the distance traveled. At a distance equal to the photon mean free path ($d=1/\mu_a$), the amount of light drops to 37% ($T=0.37$).

E. Thermal Imaging

An infrared camera (Thermacam PM250, Inframetrics, Billerica, MA) with a close-up lens was used to measure the temperature of the SMP rod upon laser heating. For these experiments, the corkscrew shape was not set and the rod was left in its straight form to eliminate movement during heating and facilitate temperature measurement along its length. Temperature distributions were observed for various ICG dye concentrations and laser powers.

F. In Vitro Thrombectomy Model

Porcine blood was obtained from a local slaughterhouse and allowed to clot (no extrinsic agents were added to accelerate clot formation). A clot was placed in a vessel model consisting of a section of clear flexible plastic tubing (lumen diameter = 6 mm) filled with water. The clot, as positioned in the tubing, was approximately 1.3 cm long and completely filled the tubing lumen diameter. The device, with the SMP microactuator in its corkscrew form, was retracted against the clot to ascertain the ability of the device to capture and hold the blood clot as the device was retracted.

G. Computer Simulation

Because laser light is used to actuate the device, its success depends on the ability of the SMP to behave as a waveguide. In its straight form, the cylindrical SMP rod suffers no leakage, much like an optical fiber. However, because laser heating must continue as the SMP changes shape, ZEMAX optical design software (ZEMAX Development Corporation, San Diego, CA) was used to model the light transmission from the optical fiber through the SMP microactuator in its corkscrew form. Light loss due to leakage out of the SMP was estimated for device actuation in air and in blood. Because the actuation occurs as the SMP transforms, modeling the light propagation in its corkscrew form represents a worst-case scenario (*i.e.,* the microactuator is initially straight when laser actuation begins).

H. Optical Fiber Bending Loss Measurement

In order to assess the feasibility of using the 100 μm core optical fiber in the tortuous paths encountered in the neurovasculature, the transmission of 800 nm laser light through a single 360° loop of the optical fiber was measured for various loop radii down to 1 mm. The amount of light exiting the looped fiber relative to the amount of light exiting the straight (no loop) fiber was measured using a power meter (LabMaster-E, Coherent, Inc., Santa Clara, CA) with a thermal sensor (LM-10, Coherent, Inc.).

I. Thermomechanical Testing of the SMP

Thermomechanical properties of the SMP were measured using dynamic mechanical thermal analysis (DMTA). DMTA measurements were made of the linear viscoelastic shear storage modulus (G') of the SMP at temperatures in the range of 25 to 120°C using an ARES LS-2 rheometer (TA Instruments, New Castle, DE). Samples were prepared by compression molding at 200°C followed by fast cooling to room temperature. Measurements were made using the torsion rectangle geometry using 50 mm long by 11 mm wide by 3.25 mm thick cut pieces. First, a strain sweep experiment was performed at 100 radians/second frequency at both room temperature and 120°C to determine the linear viscoelastic limits for strain at each temperature. Then measurements of G' were made at a frequency of 6.28 radians/second while ramping the temperature from 25 to 120°C, back down to 25°C, then up again to 120°C all at 1°C/minute while the instrument automatically adjusted the strain to maintain a linear response.

III. RESULTS

A. 800 nm Laser Light Absorption

The spectral absorption of the thermoset SMP doped with ICG dye at concentrations from 0 to 40.6 μM is shown in Fig. 5. The estimated absorption coefficient at 800 nm for the thermoplastic SMP is plotted as a function of dye concentration in Fig. 6. As expected from the Beer-Lambert Law, the absorption coefficient varies linearly with ICG concentration at the relatively low concentrations tested. The photon mean free path ($1/\mu_a$, ignoring scattering) is approximately equal to the length of the SMP rod (4 cm) at an ICG dye concentration of 0.8 μM. At this concentration, the amount of light reaching the distal end of the SMP rod has dropped to 37% (ignoring loss mechanisms other than absorption) according to equation (2). In comparison, the amount of light reaching the distal end of the SMP rod for a dye concentration of 0.08 μM is 91%.

B. Heat Distribution

Observation of the straight SMP rod during laser heating with the thermal camera showed that the axial heat distribution depended on the ICG dye concentration. Lower dye concentrations resulted in more uniform axial laser heating along the straight SMP rod. However, the temperature at the fiber-SMP joint was sometimes independent of the dye concentration, reaching unexpectedly high temperatures even at the lowest dye concentration. In some cases, the elevated temperature at the joint approached or exceeded T_g, causing irreversible deformation and/or thermal damage of the SMP, which resulted in light leakage. It is likely that laser light back-reflected from the air-SMP boundary at the end of the drilled socket (Fresnel reflection due to index mismatch) was absorbed by the epoxy, causing the temperature in the vicinity of the joint to rise excessively. To test this hypothesis, several joints were created using an index-matched optically transparent epoxy (EPO-TEK 301-2, Epoxy Technology, Inc., Billerica, MA)

applied in the socket, eliminating the air gap between the cleaved tip of the optical fiber and the SMP. Excessive heating at the joint was not evident in these samples, suggesting that the combination of the air gap and highly absorbing epoxy was responsible for the elevated temperature at the joint.

To elicit the dependence of temperature on ICG dye concentration and laser power, the temperature was measured at a point approximately 1 cm from the proximal (joint) end of the straight SMP rod for various dye concentrations as the laser power was slowly ramped up (Fig. 7). The temperature increased linearly with laser power for all dye concentrations. The linear relationship was expected since the photon energy absorbed per unit volume (and, hence, the temperature rise), E_{abs}, at a given distance, d, along the SMP rod is proportional to the product of the absorption coefficient and the power per unit area (fluence) at the given distance:

$$E_{abs} \propto \mu_a \frac{\alpha P_0}{A_{cs}} \exp(-\mu_a d) \tag{3}$$

where P_0 is the laser power output from the optical fiber, α is the fraction of light transmitted into the SMP (α<1 due to Fresnel reflection and light leakage at the air gap in the socket), and A_{cs} is the cross-sectional area of the SMP rod; the exponential accounts for the attenuation of the fluence due to absorption given by equation (2). Due to the inconsistent coupling of the laser light into the SMP (*i.e.,* the value of α potentially varied from one experiment to the next), the slopes of the curves in Fig. 7 cannot be used to determine the relative efficiency of laser heating at the various dye concentrations.

The optimal dye concentration which minimizes the amount of laser power required to heat the SMP to a given temperature can be derived theoretically. Rearranging equation (3), noting that the temperature increase, ΔT, is directly proportional to the absorbed photon energy, yields

$$P_0 \propto \frac{\Delta T A_{cs} \exp(\mu_a d)}{\alpha \mu_a} \tag{4}$$

Substituting in equation (4) the linear relationship between the absorption coefficient and the dye concentration, C, given in Fig. 6 as

$$\mu_a = 0.31C \tag{5}$$

yields the theoretical laser power needed to achieve a given temperature increase at a given distance along the SMP rod:

$$P_0 \propto \frac{1}{C} \exp(0.31Cd) \tag{6}$$

where the multiplicative constants, including ΔT, have been absorbed into the proportionality symbol. Equation (6) is plotted as a function of ICG dye concentration for various distances in Fig. 8. Isolating P_0 in equation (3) and setting $dP_0/d\mu_a$ (derivative of P_0 with respect to μ_a) equal to zero yields a minimum of P_0 at $\mu_a = 1/d$. Again using the linear relationship between the dye concentration and the absorption coefficient given in Fig. 6 and equation (5), P_0 is minimized when the dye concentration is equal to $1/(0.31d)$. Note that this dye concentration is independent of the desired temperature increase; that is, this dye concentration will require the least amount of laser power to achieve any given temperature (*e.g.,* T_{gs}) at a distance, d, along the SMP rod. For the 4 cm long SMP rod, the most efficient use of laser power occurs at a dye concentration of 0.8 μM (minimum laser power required to achieve a given temperature rise at $d = 4$ cm).

Because more laser power is needed to achieve actuation of the SMP distally (farther from the fiber-SMP joint) versus proximally, a laser power must be chosen to achieve sufficient heating distally. As a result, proximal temperatures are higher than necessary. A non-uniform dye concentration in which the concentration gradually increased with distance from the joint would require less laser power and result in a more uniform axial temperature distribution. The optimal axial concentration profile is determined by using the relationship between P_0 and the dye concentration, C, as given in equation (6):

$$P_0^{\min} \propto \frac{1}{C}\exp(0.31Cd) = 3.37 \tag{7}$$

where $P_0^{\min} = 3.37$ is the minimum value of P_0 at $d = 4$ cm, obtained by evaluating the expression in equation (6) at $C = 1/(0.31d)$, where $d = 4$. Fig. 9 shows the dye concentration versus distance along the SMP rod obtained by numerically solving equation (7). This axial concentration profile would theoretically result in uniform axial heating of the SMP rod using the least amount of laser power.

C. Laser Actuation

Successful laser actuation of the SMP device (*i.e.,* complete recovery of the primary corkscrew shape) was achieved in air at ICG dye concentrations from 0.08 to 1.56 μM using laser powers from approximately 900 to 1100 mW. Higher and lower dye concentrations were not tested. Due to the excessive heating at the fiber-SMP joint, intermittent failures (partial or no actuation due to thermal deformation or damage of the SMP) also occurred at these dye concentrations. Snapshots of a successful actuation attempt taken at 1-second intervals are shown in Fig. 10. Full deployment from the straight rod to the corkscrew shape occurred within 5 seconds.

D. In Vitro Thrombectomy

The SMP microactuator in its corkscrew form was able to pull porcine blood clots through the vessel model a distance up to 15 cm, at which point the end of the tubing was

reached. The SMP microactuator either remained distal to the clot during retraction of the device (only the first turn of the corkscrew was engaged in the clot) or pulled into the clot such that several turns of the corkscrew held the clot.

E. Computer Simulation

A three-dimensional ray trace diagram illustrating light propagation through the SMP corkscrew in air is shown in Fig. 11(a). An air gap of 0.01 mm in the drilled socket between the cleaved tip of the optical fiber and the SMP was modeled, but the convex nature of the socket was not (it was assumed to be flat). Most of the 20 randomly selected light rays emitted by the optical fiber (numerical aperture = 0.22) exit the SMP at the distal end, though some leak out early. Virtual detectors were placed along the SMP to monitor the amount of light at each location on the corkscrew. Fig. 11(b) provides a comparison of the amount of light loss versus distance along the corkscrew in air (index of refraction = 1.00) and blood (index of refraction = 1.38 [8]) with and without an air gap in the drilled socket. The higher index of refraction of blood results in increased light leakage. However, filling the air gap with a transparent material whose index of refraction matches that of the SMP (estimated to be 1.56 at 800 nm) reduces the amount of loss. The simulations suggest that elimination of the air gap will compensate for the negative effect of blood on the waveguiding ability of the SMP corkscrew.

F. Optical Fiber Performance

The transmission of 800 nm laser light through the optical fiber with a single 360° loop versus loop curvature is shown in Fig. 12. Approximately 80% of the light is transmitted for a loop radius of 4 mm, and over 90% of the light is transmitted when the radius is increased to 6 mm.

G. Thermomechanical Behavior of the SMP

The dynamic storage (elastic) modulus (G') of the SMP measured by DMTA is shown in Fig. 13. At 37°C (body temperature), the elastic modulus (E) of the SMP, given by $E \approx 2.8G'$, is approximately 2400 MPa. As the SMP is heated, E falls to approximately 44 MPa near its soft phase glass transition temperature (55°C), and eventually drops as low as 4 MPa. Finally, after cooling back to 37°C, E approaches its original value though there is some hysteresis and the actual value reaches only about 80% of the prior value.

IV. DISCUSSION

A. Nonpharmacologic Alternatives to rt-PA

The narrow treatment window, combined with the risk of intracranial hemorrhage following rt-PA administration, has prompted development of alternative, nonpharmacologic treatment methods for ischemic stroke [9]. Clinical studies investigating localized intra-arterial thrombolytic drug treatment have demonstrated neurological benefit in patients treated up to 6 hours after symptom onset [10], [11]. Such findings suggest the treatment window for mechanical thrombus removal may extend well beyond the current 3-hour limit imposed by rt-PA. In addition, mechanical thrombus removal is potentially faster than the chemical process of thrombolysis, occurring on the order of minutes rather than hours. Furthermore, because there is no systemic drug exposure, complications, contraindications, and the need for follow-up patient care associated with conventional thrombolytic drug administration are reduced or eliminated.

Recent human studies indicate that mechanical thrombus removal following acute ischemic stroke is potentially safer, faster, and, because it may extend the treatment time window and reduce complications, more effective than conventional thrombolytic treatment. Early clinical trials have demonstrated the safety and feasibility of laser thrombolysis, an intra-arterial technique which emulsifies the thrombus photoacoustically, in patients treated up to 6 hours (anterior occlusion) and 24 hours (posterior occlusion) after symptom onset [9], [12]. Successful rheolytic thrombectomy using high-pressure saline jets to fragment and aspirate the thrombus in the internal carotid artery within 3-6 hours after symptom onset has also been reported [9], [13]. In addition, pilot studies of various other mechanical devices, including a rotating cutting device, have been initiated [9].

Of particular interest is a metal wire device recently approved by the Food and Drug Administration to mechanically retrieve the thrombus up to 8 hours after the onset of stroke [9], [14]. This device, known as the Merci® Retriever (Concentric Medical, Inc., Mountain View, CA), is used to physically capture the thrombus in a manner similar to our SMP device concept. The wire is made of a nickel-titanium shape memory alloy (nitinol) and has a primary corkscrew form. The device is delivered via a balloon guide catheter and the balloon is inflated to control antegrade flow. The nitinol wire is sheathed by a microcatheter as it is pushed distally over a guide wire through the thrombus. The guide wire and microcatheter are then retracted, exposing the nitinol wire and allowing it to resume its corkscrew form and capture the thrombus. The thrombus is then pulled back to the tip of the balloon guide catheter where it is aspirated.

In addition to the use of polymer versus metal, a major difference between our device concept and the Merci® Retriever is that our device is being designed to traverse the neurovasculature and penetrate the thrombus without an overlying microcatheter. This feature eliminates the need to use to guide wire to pass the device through the thrombus. Actual device performance will be elucidated in future animal studies, which will provide

a more substantial means for comparison to the Merci® Retriever and other thrombectomy devices.

B. SMP Microactuator: Current Status and Future Directions

A basic framework for the SMP microactuator device has been established. We have demonstrated laser actuation of the SMP corkscrew device in a nonphysiologic environment: air at room temperature. Optical computer simulations indicated that deployment in blood is also feasible. Viable ICG dye concentrations and laser powers were determined using spectrophotometry and thermal imaging in air. In a blood environment at body temperature, significantly more laser power would be required to achieve thermal actuation of the SMP microactuator due to the cooling effect of the surrounding blood compared to deployment in air. Assuming heat transfer is limited to conduction (no fluid flow) as a first approximation, heat transfer from the SMP microactuator to the surrounding fluid (air or blood) can be described by Fourier's law [15]:

$$q = -k\Delta T/\Delta L \tag{8}$$

where q is the rate of energy transfer per unit area, k is the thermal conductivity of the fluid, ΔT is the difference between the temperature of the SMP surface and the temperature of the fluid at a point away from the surface in the steady state, and ΔL is the distance from the SMP surface to the point in the fluid away from the surface. The relative amounts of laser power required to maintain the SMP surface at its glass transition (actuation) temperature of 55°C for laser heating in room temperature (22°C) air (k_{air}=0.026 W/m-K [16]) versus body temperature (37°C) blood (k_{blood}=0.53 W/m-K [15]) can be estimated from the ratio of the respective q values using equation (8):

$$\frac{q_{blood}}{q_{air}} = \frac{k_{blood}\left(T_{SMP} - T_{blood}\right)}{k_{air}\left(T_{SMP} - T_{air}\right)} \tag{9}$$

Substituting the thermal conductivity and steady state temperature values into equation (9) indicates that roughly 11 times more laser power is needed to achieve actuation in the blood environment. Despite the discrepancy between laser powers for actuation in air and blood, the thermal images acquired in air nevertheless provided a useful means of characterizing the relative temperature of the SMP microactuator for various laser powers. Actual laser power needed to achieve actuation in blood will be determined empirically.

Though not all of the benchtop laser actuation tests were successful, further experimental testing and computer simulation enabled identification of the cause of inconsistent operation of the device: overheating of the epoxy due to absorption of back-reflected laser light at the air gap in the socket at fiber-SMP interface. Preliminary testing in an *in vitro* vessel model demonstrated the ability of the SMP corkscrew to retrieve a clot. Though this simplified model did not address the tortuous geometry that could be

encountered in the human neurovasculature, it did provide useful insight for future testing in more complicated systems and animal models. Feasibility of the optical fiber under the tortuous paths of the neurovasculature was confirmed.

The stiffness of the SMP microactuator was quantified by measurement of the elastic modulus. During laser heating, the elastic modulus of the SMP drops significantly, rendering the microactuator quite flexible as the corkscrew is formed, until the laser is turned off and the SMP cools. Due to the hysteresis upon cooling, the elastic modulus of the microactuator at body temperature after it has been heated to form the corkscrew is about 20% less than that of the microactuator in its initial straight rod form. The elastic modulus of the SMP at body temperature, both before (straight rod form) and after (corkscrew form) laser actuation, is more than an order of magnitude lower than that of nitinol [17] used in the Merci® device described previously. However, the actual flexibility of the devices depends on their geometries as well as their elastic moduli. Because our SMP device is being designed to traverse the vasculature and pass through the thrombus without the need to first place a guide wire, a more flexible extension of the SMP microactuator will be incorporated to lessen dependence of the maneuverability on the flexibility of the SMP. Such an extension can be made of polymers with elastic moduli as low as 0.5 MPa, or can consist of tightly coiled fine metal wire similar to a standard guide wire tip.

Development of the device is ongoing. Use of an optically transparent index-matched epoxy in the socket eliminated the air gap and resolved the problem of joint overheating. To further refine the fiber-SMP joint, we have successfully used an excimer laser to create the socket in the SMP. The socket surface is flat, permitting better approximation between the SMP surface and the optical fiber tip. Based on the calculation of optimal dye concentration, a gradually increasing dye concentration along the SMP rod would yield the most efficient laser heating (*i.e.,* uniform axial heating profile), enabling laser actuation using lower laser powers than those reported in this study. Other refinements that are currently being developed include: (i) a flexible distal extension of the SMP microactuator to facilitate negotiation of the neurovasculature, (ii) a torqueable sheath around the optical fiber to enhance strength and maneuverability through tortuous vessels, (iii) radio-opaque markers for fluoroscopic guidance, and (iv) a secondary means of securing the thrombus for removal from the body after capture. Additionally, the corkscrew diameter may be reduced depending on the size of the target vessel. Improvements such as these will facilitate future testing under physiologic conditions and in animal models. This preliminary study suggests that the SMP microactuator for mechanical thrombus removal is a promising therapeutic alternative for acute ischemic stroke.

ACKNOWLEDGMENT

The authors wish to thank B. Kelly and D. Schumann for their technical assistance in fabricating the devices.

REFERENCES

[1] National Institute of Neurological Disorders and Stroke rt-PA Stroke Study Group, "Tissue plasminogen activator for acute ischemic stroke," *N. Engl. J. Med.*, vol. 333, pp. 1581-1587, 1995.

[2] J. R. Marler, B. C. Tilley, M. Lu, T. G. Brott, P. C. Lyden, J. C. Grotta, J. P. Broderick, S. R. Levine, M. P. Frankel, S. H. Horowitz, E. C. Haley, Jr., C. A. Lewandowski, and T. P. Kwiatkowski, "Early stroke treatment associated with better outcome: the NINDS rt-PA stroke study," *Neurology*, vol. 55, pp. 1649-1655, 2000.

[3] W. M. Clark, S. Wissman, G. W. Albers, J. H. Jhamandas, K. P. Madden, and S. Hamilton, "Recombinant tissue-type plasminogen activator (Alteplase) for ischemic stroke 3 to 5 hours after symptom onset. The ATLANTIS study: a randomized controlled trial. Alteplase thrombolysis for acute noninterventional therapy in ischemic stroke," *JAMA*, vol. 282, pp. 2019-2026, 1999.

[4] R. E. O'Connor, P. McGraw, and L. Edelsohn, "Thrombolytic therapy for acute ischemic stroke: why the majority of patients remain ineligible for treatment," *Ann. Emerg. Med.*, vol. 33, pp. 9-14, 1999.

[5] D. J. Maitland, M. F. Metzger, D. Schumann, A. Lee, and T. S. Wilson, "Photothermal properties of shape memory polymer micro-actuators for treating stroke," *Lasers Surg. Med.*, vol. 30, pp. 1-11, 2002.

[6] M. F. Metzger, T. S. Wilson, D. Schumann, D. L. Matthews, and D. J. Maitland, "Mechanical properties of mechanical actuator for treating ischemic stroke," *Biomedical Microdevices*, vol. 4, pp. 89-96, 2002.

[7] B. Henderson, "Optical spectrometers," in *Handbook of Optics Volume II*, M. Bass, E. W. Van Stryland, D. R. Williams, and W. L. Wolfe, Eds. New York: McGraw-Hill, 1995.

[8] D. K. Sardar and L. B. Levy, "Optical properties of whole blood," *Lasers Med. Sci.*, vol. 13, pp. 106-111, 1998.

[9] M. C. Leary, J. L. Saver, Y. P. Gobin, R. Jahan, G. R. Duckwiler, F. Vinuela, C. S. Kidwell, J. Frazee, and S. Starkman, "Beyond tissue plasminogen activator: mechanical intervention in acute stroke," *Ann. Emerg. Med.*, vol. 41, pp. 838-846, 2003.

[10] G. J. del Zoppo, R. T. Higashida, A. J. Furlan, M. S. Pessin, H. A. Rowley, M. Gent, and the PROACT Investigators, "PROACT: a phase II randomized trial of recombinant pro-urokinase by direct arterial delivery in acute middle cerebral artery stroke," *Stroke*, vol. 29, pp. 4-11, 1998.

[11] A. Furlan, R. Higashida, L. Wechsler, M. Gent, H. Rowley, C. Kase, M. Pessin, A. Ahuja, F. Callahan, W. M. Clark, F. Silver, and F. Rivera, "Intra-arterial prourokinase for acute ischemic stroke. The PROACT II study: a randomized controlled trial. Prolyse in acute cerebral thromboembolism," *JAMA*, vol. 282, pp. 2003-2011, 1999.

[12] H. L. Lutsep, M. Campbell, W. M. Clark, O. Jansen, M. A. Lefkowitz, M. P. Marks, A. Norbash, C. Putnam, and M. Schumacher, "EPAR therapy system for treatment of acute stroke: safety study results [abstract]," *Stroke*, vol. 32, p. 319-b, 2001.

[13] R. J. Bellon, C. M. Putman, R. F. Budzik, R. S. Pergolizzi, G. F. Reinking, and A. M. Norbash, "Rheolytic thrombectomy of the occluded internal carotid artery in the setting of acute ischemic stroke," *AJNR Am. J. Neuroradiol.*, vol. 22, pp. 526-530, 2001.
[14] Y. P. Gobin, S. Starkman, G. R. Duckwiler, T. Grobelny, C. S. Kidwell, R. Jahan, J. Pile-Spellman, A. Segal, F. Vinuela, and J. L. Saver, "MERCI 1: A phase 1 study of mechanical embolus removal in cerebral ischemia," *Stroke*, vol. 35, pp. 2848-2854, 2004.
[15] C.-S. Orr and R. C. Eberhart, "Overview of bioheat transfer," in *Optical-Thermal Response of Laser Irradiated Tissue*, A. J. Welch and M. J. C. van Gemert, Eds. New York: Plenum Press, 1995.
[16] D. Halliday and R. Resnick, *Fundamentals of Physics*. New York: John Wiley and Sons, 1988, ch. 20.
[17] M. P. Walker, R. J. White, and K. S. Kula, "Effect of fluoride prophylactic agents on the mechanical properties of nickel-titanium-based orthodontic wires," *Am. J. Orthod. Dentofacial Orthop.*, vol. 127, pp. 662-669, 2005.

Ward Small IV received the B.S. degree in Engineering Physics in 1993 from the University of California, San Diego, and the Ph.D. degree in 1998 from the University of California, Davis, where he studied laser-tissue interaction and biomedical optical diagnostics in support of the laser tissue welding effort in the Medical Technology Program at Lawrence Livermore National Laboratory.

He spent five years in the pharmaceutical industry with Miravant Medical Technologies investigating the use of light-activated photodynamic therapy drugs for treating ophthalmic and dermatologic diseases before joining the Medical Physics and Biophysics Division at Lawrence Livermore National Laboratory in 2003. His current research interests include photomechanical intravascular device development and second harmonic generation microscopy.

Melodie F. Metzger received the B.S. degree in Bioengineering from the University of California, Berkeley in 2001.

From 2001 to 2003 she investigated biomedical applications of shape memory polymers in the Medical Physics and Biophysics Division at Lawrence Livermore National Laboratory. In 2003 she founded Sierra Interventions, LLC, specializing in the creation of novel minimally invasive, intravascular medical devices. She is currently pursuing a Ph.D. degree in Bioengineering at the University of California, Berkeley.

Thomas S. Wilson received the B.S. degree in 1985 from the University of Wisconsin, Madison, and the Ph.D. degree in 1991 from Virginia Polytechnic Institute and State University, both in Chemical Engineering.

He was with Rohm and Hass Company from 1991 to 2000 where he focused on the characterization of rheological, thermal, and physical properties of polymeric materials with application to new material development and material processing. Since 2000, he has worked in the Medical Physics and Biophysics Division at Lawrence Livermore National Laboratory. His current research interests include synthesis and characterization

of new shape memory polymers, hydrogels, and biomaterials for medical devices, biosensors, and artificial organs.

In 2002, Dr. Wilson became an Assistant Clinical Professor in the Medical Division of Internal Medicine at the University of California, Davis. He is a member of the American Chemical Society, the Society of Plastics Engineers, and the Society of Rheology.

Duncan J. Maitland received the B.S. degree in Electrical Engineering in 1985 and the M.S. degree in Physics in 1989, both from Cleveland State University. He received the Ph.D. degree in Bioengineering from Northwestern University in 1995.

From 1985 to 1987 he was a flight control systems engineer at Goodyear Aerospace before joining NASA Glenn (formerly Lewis) Research Center, where he built and tested prototype fiber optic sensors for aircraft engines until 1989. Since 1995 he has been with Lawrence Livermore National Laboratory, where he has served as Group Leader of the Medical Technology Program and Associate Division Leader of the Medical Physics and Biophysics Division. His current research interests include therapeutic laser-tissue interactions, interventional endovascular device development and vascular fluid dynamics and thermal transport.

Dr. Maitland has served as a reviewer for *Applied Optics*, *Optics Letters*, *Journal of Biomedical Optics*, and *Lasers in Surgery and Medicine*, and is a member of the National Institutes of Health Bioengineering and Physiology Study Section. He has 35 publications and 7 granted patents.

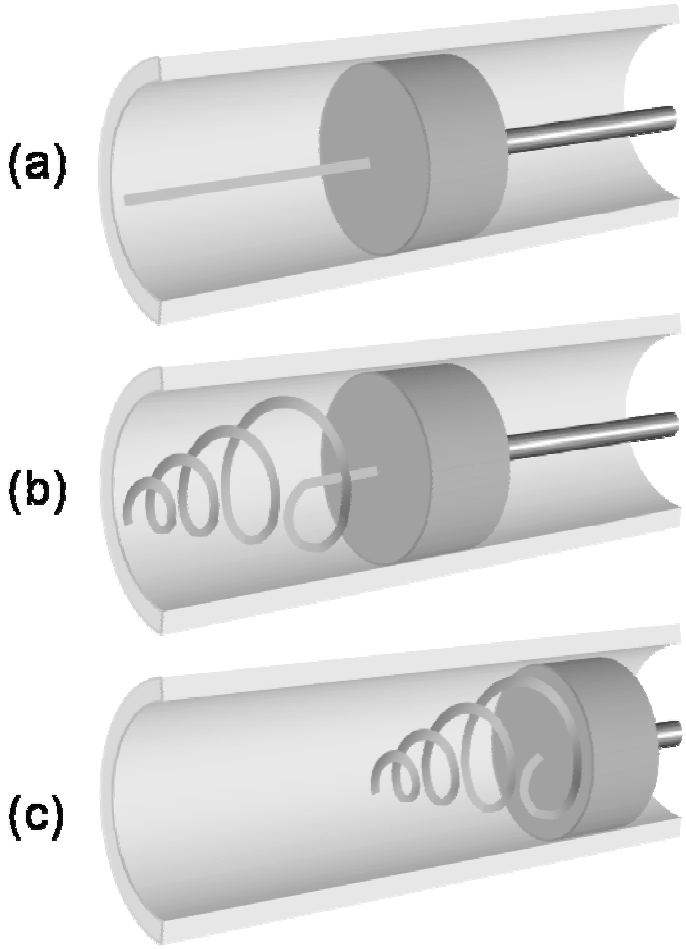

Fig. 1. Depiction of endovascular thrombus removal using the SMP microactuator. (a) In its secondary straight rod form, the microactuator is delivered through a catheter distal to the vascular occlusion. (b) The microactuator, which is mounted on the end of an optical fiber, is then transformed into its primary corkscrew shape by laser heating. (c) Once deployed, the microactuator is retracted and the captured thrombus is removed to restore blood flow.

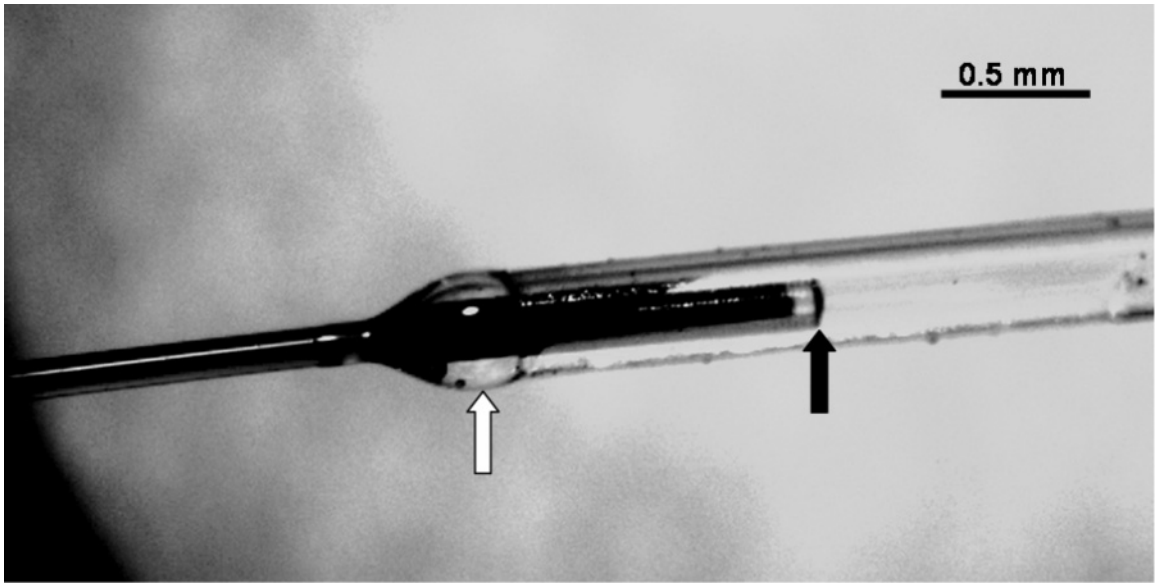

Fig. 2. Microscope image of the fiber-SMP joint. The cleaved end of the optical fiber is inserted into the drilled socket in the SMP rod. The glass core of the fiber is slightly exposed at the cleaved end where the polyimide buffer was removed prior to cleaving. The convex shape of the socket and resulting air gap where it meets the cleaved fiber tip are apparent (black arrow). Epoxy applied external to the socket (white arrow) secures the joint.

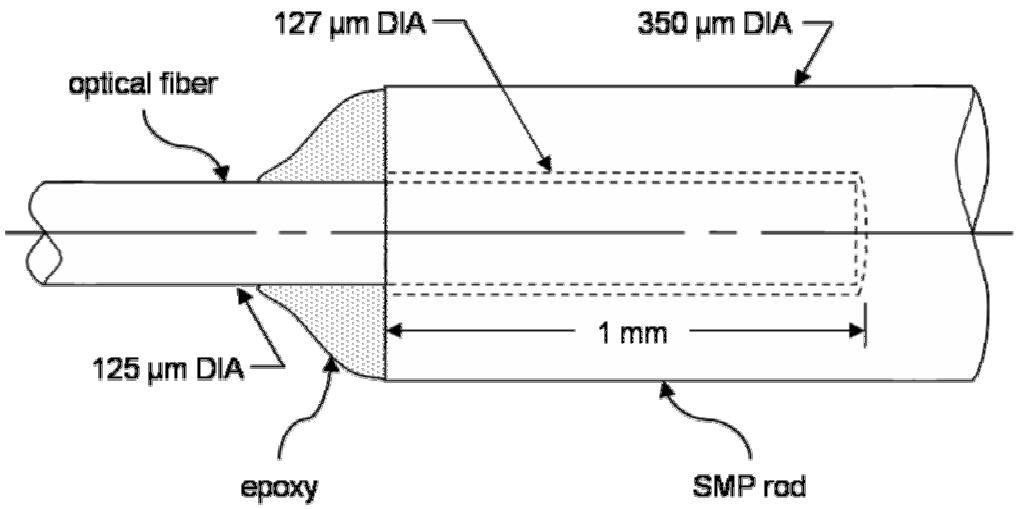

Fig. 3. Configuration of the SMP-fiber joint. The cleaved end of the optical fiber is inserted into a coaxial socket in the SMP rod and bonded in place with epoxy. Because the drill bit used to created the socket yielded a slightly convex surface at the end of the socket, a small air gap exists between the cleaved fiber tip and the SMP. Some epoxy typically migrates slightly into the socket before curing (not shown). Drawing not exactly to scale.

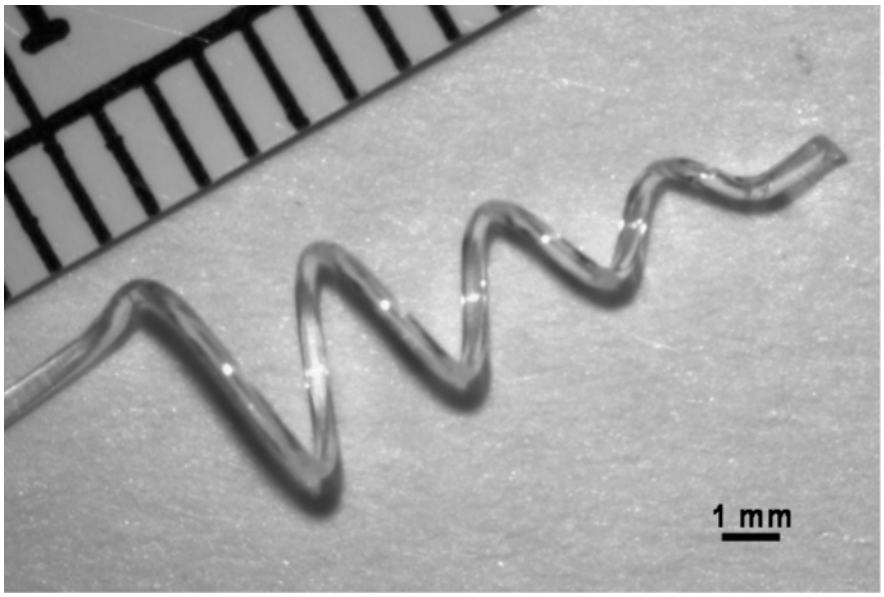

Fig. 4. SMP microactuator in its corkscrew form. The proximal (joint) end is to the left (joint not shown). When straightened, the SMP is approximately 4 cm in length.

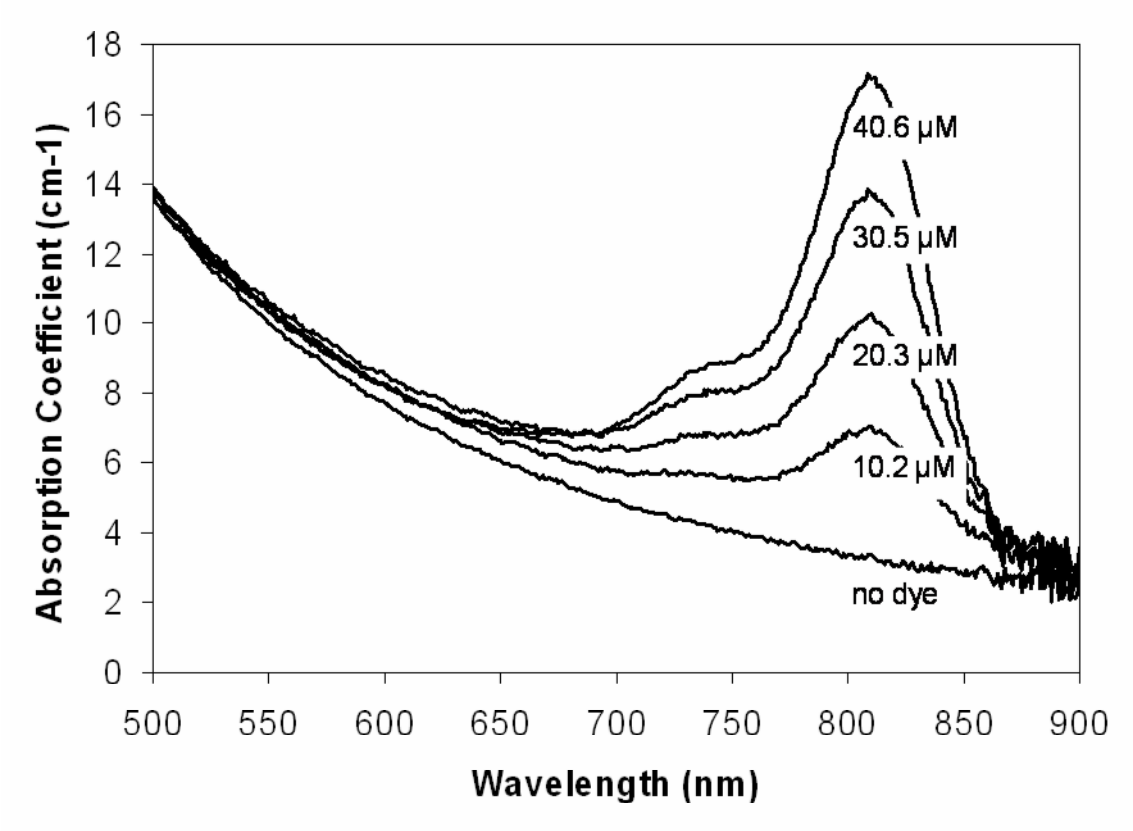

Fig. 5. Spectral absorption of thermoset SMP doped with ICG dye. Dye concentrations of 10.2, 20.3, 30.5, and 40.6 µM were tested. Thermoset SMP with no dye was also tested.

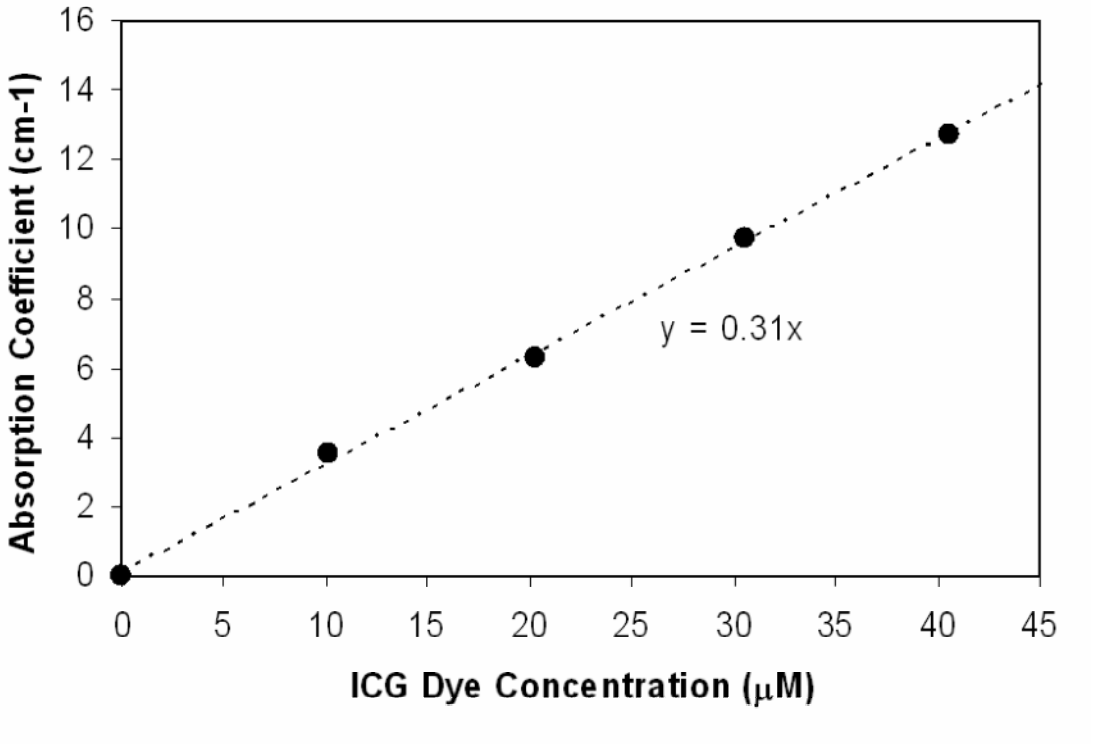

Fig. 6. Estimated absorption coefficient at 800 nm for thermoplastic SMP versus ICG dye concentration (data points). Dye concentrations of 0 (no dye), 10.2, 20.3, 30.5, and 40.6 μM were tested. A linear relationship exists between the absorption coefficient and dye concentration.

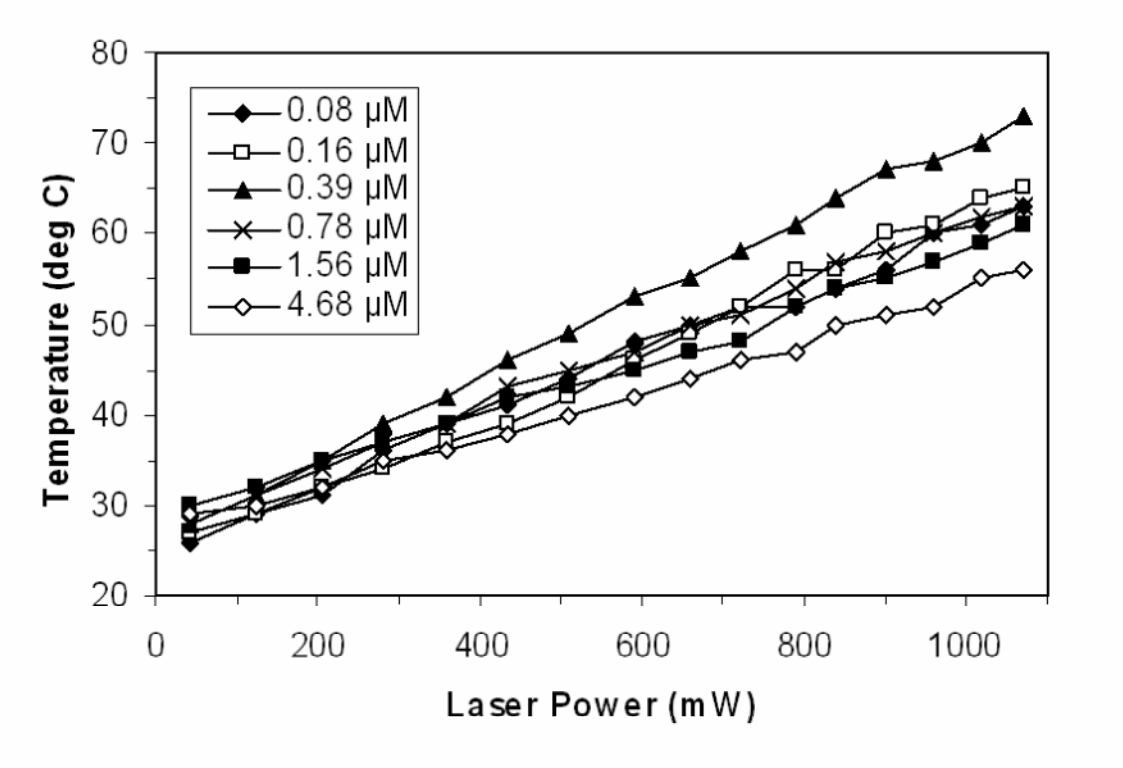

Fig. 7. Temperature 10 mm from the proximal (joint) end of the straight SMP rod versus laser power for ICG dye concentrations from 0.08 to 4.68 µM (data points). The temperature increased with laser power in a linear fashion for all dye concentrations.

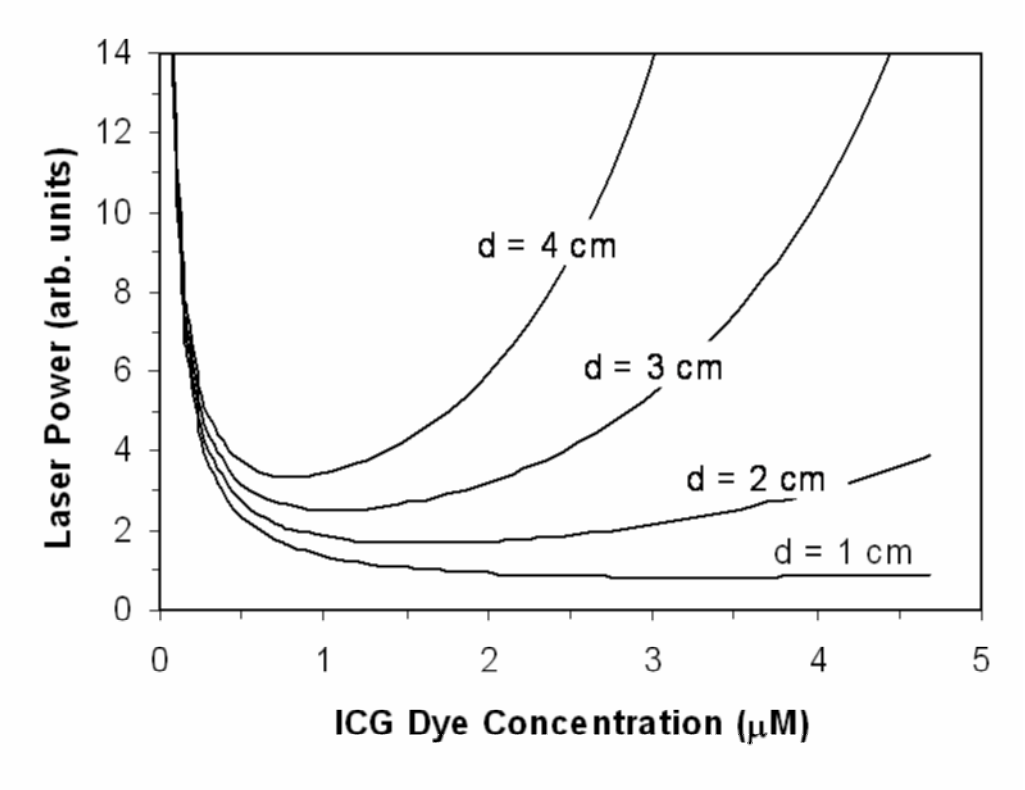

Fig. 8. Theoretical laser power required to achieve a given temperature increase versus ICG dye concentration at a distance of 1, 2, 3, or 4 cm from the proximal (joint) end of the straight SMP rod. For the 4 cm long SMP rod, the most efficient use of laser power occurs at a dye concentration of 0.8 μM (minimum laser power required to achieve a given temperature rise at d = 4 cm).

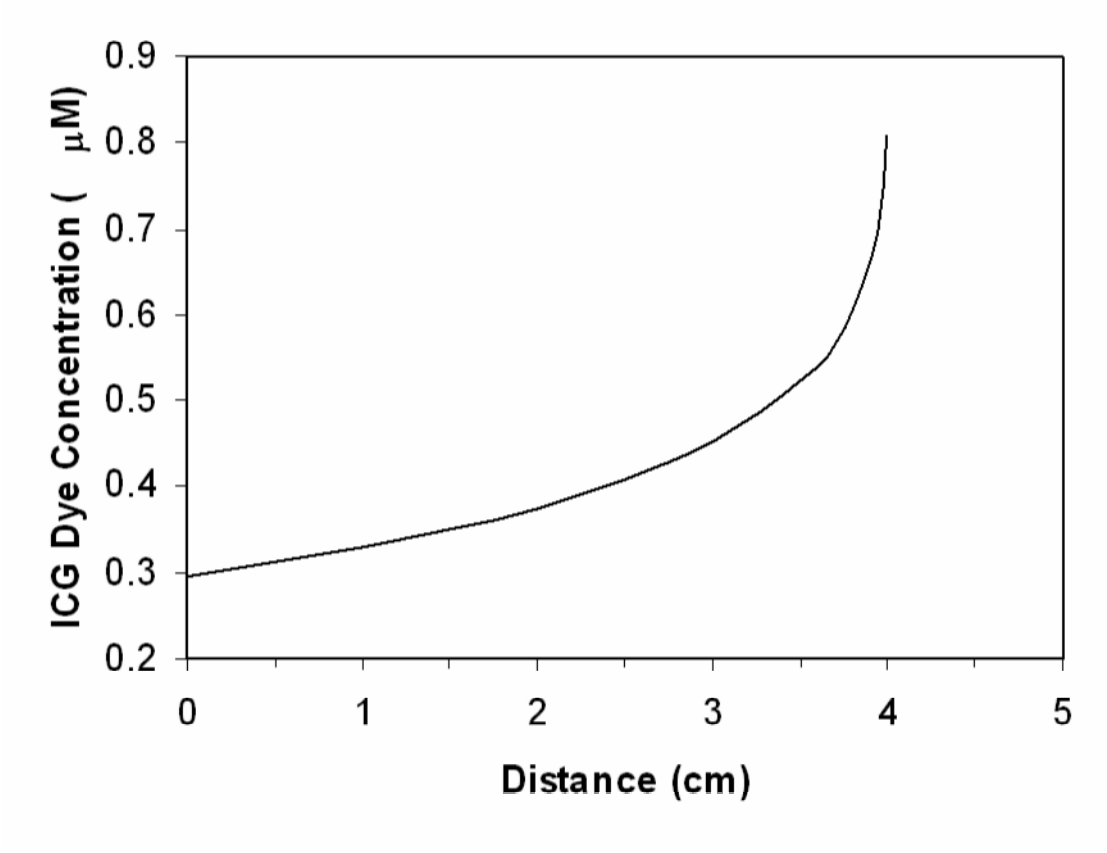

Fig. 9. Theoretical axial ICG dye concentration profile yielding uniform heating of the SMP rod using the least amount of laser power. As more laser energy is absorbed as the light propagates through the SMP rod, more dye is required to maintain a constant temperature.

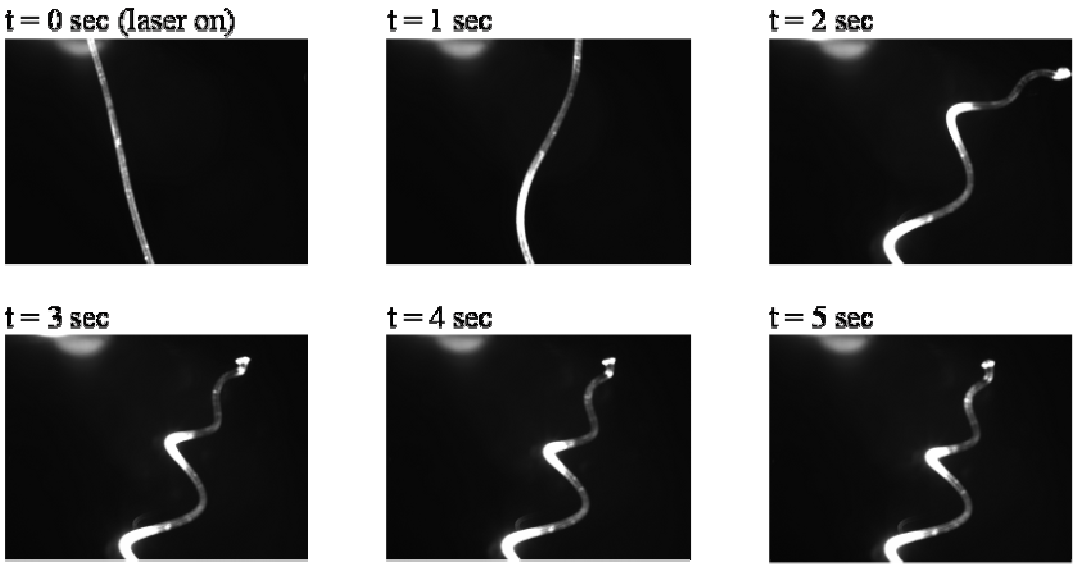

Fig. 10. Laser-activated SMP microactuator deployment sequence. Full deployment from straight rod to corkscrew occurs within 5 seconds. The length of the SMP microactuator is 4 cm in its initial straight form. The ICG concentration was 0.08 μM. The laser power was approximately 1000 mW.

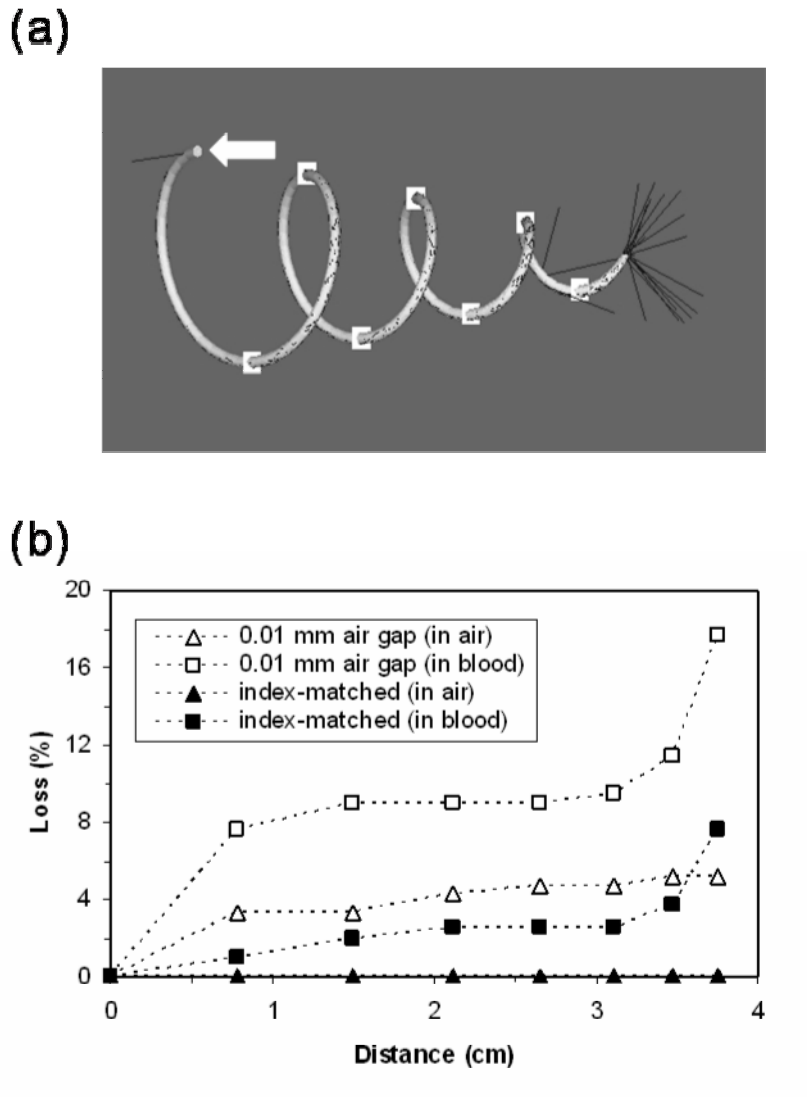

Fig. 11. (a) ZEMAX three-dimensional ray trace diagram of laser light propagation through the SMP microactuator in its corkscrew shape. The optical fiber (not pictured) enters the SMP at the end of the corkscrew indicated by the arrow. This ray trace was generated for a 0.01 mm air gap in the drilled socket between the cleaved tip of the optical fiber and the SMP assuming the SMP device is in air. Virtual detectors placed along the corkscrew monitored the amount of light at each location to determine the effect of filling the air gap with a material with the same index of refraction as the SMP, as shown in (b). The percentage of light loss is plotted against distance along the corkscrew (data points). Additional simulations were performed to assess the waveguiding ability of the SMP device in blood. Surrounding the device with blood increased light leakage, but elimination of the air gap compensated for the extra loss.

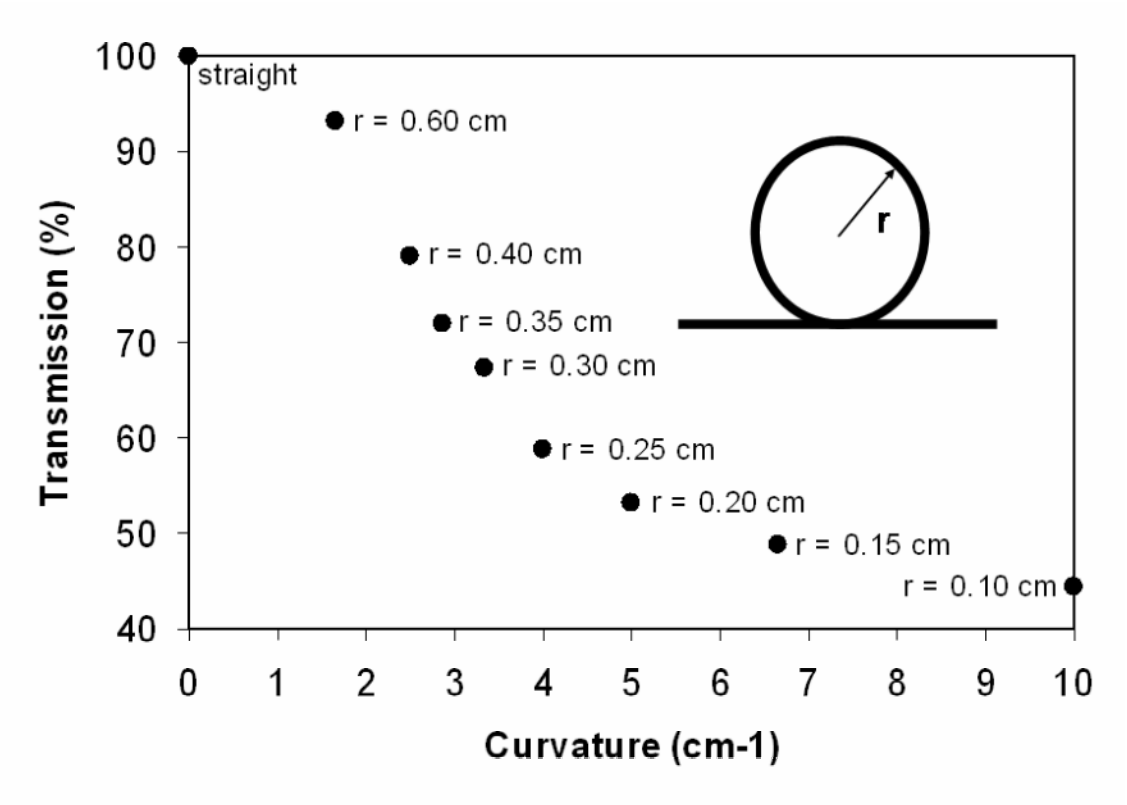

Fig. 12. Transmission of 800 nm laser light through the 100 μm core optical fiber with a single 360° loop plotted as a function of loop curvature, 1/r (data points). The transmission exceeds 90% for loop radii above 6 mm. The transmission drops to 80% at a loop radius of 4 mm.

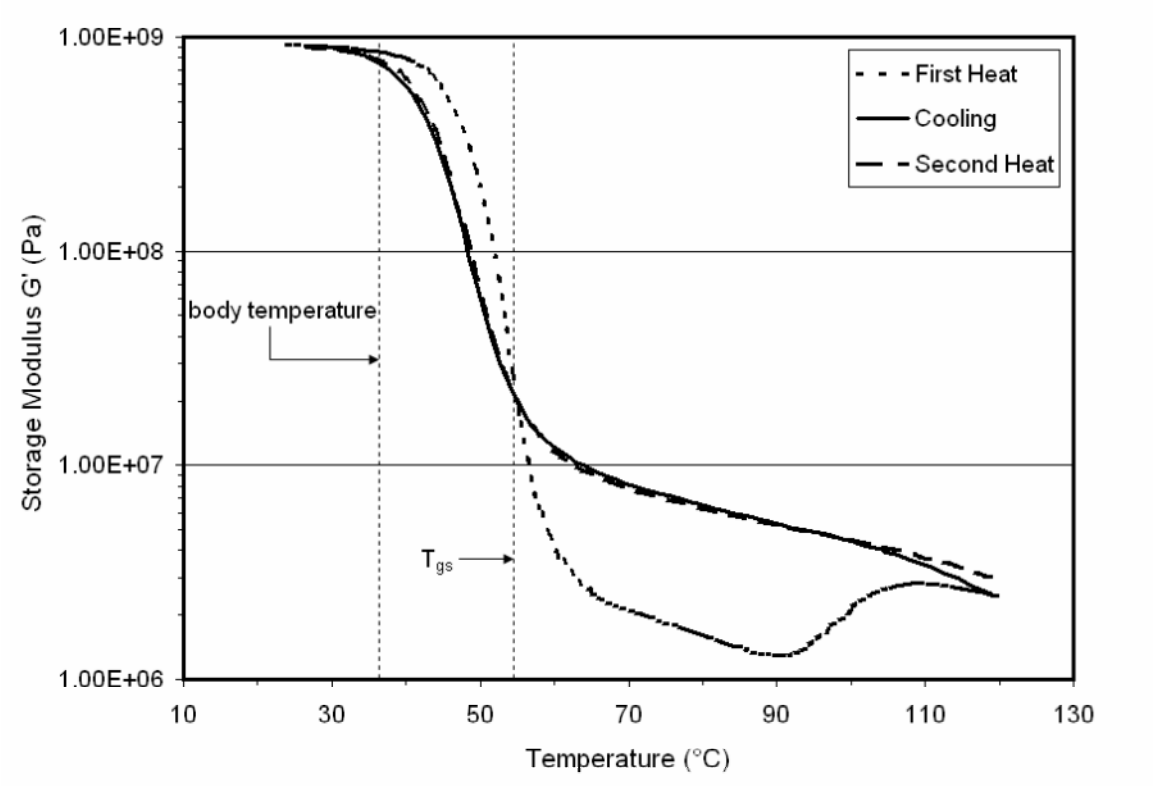

Fig. 13. Storage modulus (G') of the SMP plotted as a function of temperature. The SMP sample underwent an initial heating phase, followed by a cooling phase, and then a second heating phase. Body temperature (37°C) and the nominal soft phase glass transition (actuation) temperature of the SMP (T_{gs}=55°C) are indicated for reference.